Motion of Liquid Drops on Surfaces Induced by Asymmetric Vibration: Role of Contact Angle Hysteresis

ARTICLE *in* LANGMUIR · AUGUST 2011

Impact Factor: 4.46 · DOI: 10.1021/la201597c · Source: PubMed

2 AUTHORS:

Srinivas Mettu
University of Melbourne
17 PUBLICATIONS **193** CITATIONS

SEE PROFILE

Manoj K. Chaudhury
Lehigh University
154 PUBLICATIONS **9,252** CITATIONS

SEE PROFILE

Langmuir

ARTICLE

pubs.acs.org/Langmuir

Motion of Liquid Drops on Surfaces Induced by Asymmetric Vibration: Role of Contact Angle Hysteresis

Srinivas Mettu and Manoj K. Chaudhury*

Department of Chemical Engineering, Lehigh University, Bethlehem, Pennsylvania 18015, United States

ABSTRACT: Hysteresis of wetting, like the Coulombic friction at solid/solid interface, impedes the motion of a liquid drop on a surface when subjected to an external field. Here, we present a counterintuitive example, where some amount of hysteresis enables a drop to move on a surface when it is subjected to a periodic but asymmetric vibration. Experiments show that a surface either with a negligible or high hysteresis is not conducive to any drop motion. Some finite hysteresis of contact angle is needed to break the periodic symmetry of the forcing function for the drift to occur. These experimental results are consistent with simulations, in which a drop is approximated as a linear harmonic oscillator. The experiment also sheds light on the effect of the drop size on flow reversal, where drops of different sizes move in opposite directions due to the difference in the phase of the oscillation of their center of mass.

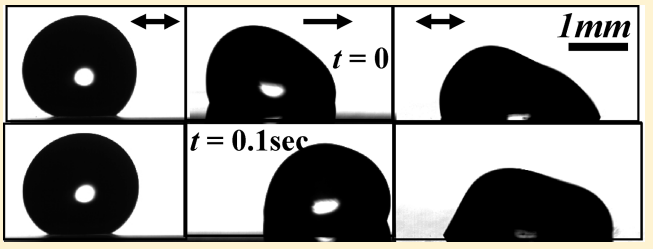

INTRODUCTION

Directed motion of a liquid drop on a solid substrate is not only an interesting phenomenon of fluid physics, it is of potential importance in applications ranging from microfluids[1−6] to heat transfer devices.[7−9] Recently, Daniel et al.[1] observed that a sessile liquid drop exhibits a net drift on a solid substrate when it is subjected to a periodic but asymmetric vibration. Later, in some interesting experiments, Brunet et al.[10] and Noblin et al.[11] observed the climbing of a drop on an inclined plane when an asymmetry is imposed by coupling horizontal and vertical vibrations. It has been understood that, for any type of motion to occur under a periodic or stochastic forcing, some kind of nonlinearity is required that breaks the symmetry of the applied force. Quite a while ago, Mogilner et al.[12] proposed such a concept in the context of the ratcheting motion of protein motors due to thermal fluctuations. Mogilner et al.[12] suggested that unidirectional motion of a protein motor is possible if the asymmetric velocity fluctuations resulting form the conformational changes of the protein are rectified by a Coulombic-type friction. Recent theoretical study of Cebiroglu et al.[13] suggested that rectified motion can also be achieved in nonlinear media subjected to asymmetric random driving. An excellent review by Hanggi and Marchesoni[14] discusses the mechanism of rectified transport at various scales in the presence of a stochastic or a deterministic driving. In the context of the drop motion, the suggestion of Daniel et al.[1−3] is similar to that of Mogilner et al.[12] Recently, Buguin et al.[15] and Fleishman et al.[16] expanded these arguments to describe the motion of a solid object on another where a Coulombic dry friction operates. Experimental demonstrations of the motion of a solid on another solid by asymmetric vibration and friction were provided by Mahadevan et al.[17] and Eglin et al.,[18] as well as by Buguin et al.[15]

For a liquid drop, no motion is expected in the steady state, other than the initial transient state, if only a linear kinematic friction acts on it. Brunet et al.[10] invoked an empirical nonlinear friction model that is perceived to be different from hysteresis in order to describe the uphill motion of a drop when vibrated strongly. John and Thiele[19,20] pointed out that the vibration component of the drop perpendicular to the substrate leads to a strongly nonlinear lateral force−velocity relation that breaks the symmetry of the periodic forcing, which is behind the effect studied by Brunet et al.[10] and Noblin et al.[11] Upon the basis of the suggestions of these authors, a question arises as to whether hysteresis is at all the necessary nonlinearity for the drop motion under asymmetric vibration in the types of experiments presented by Daniel et al.[1]

The fact that hysteresis can play a role in the ratcheting motion has been evident in another related study of Daniel et al.,[3] in which a liquid drop was periodically squeezed and extended between two surfaces with a very low frequency (1 Hz) vibration. Here, both the supporting substrate with a wettability gradient as well as the upper substrate (with no wettability gradient) that deforms the drop had finite hysteresis. This experiment showed that a ratcheting motion of a drop readily occurs due to contact angle hysteresis. More recently, Prakash et al.[21] discovered an interesting parallel in the water feeding behavior of Phalarope shore birds, the explanation of which is same as that proposed earlier by Daniel et al.[3]

Now, central to the argument of whether or not hysteresis can play a role in the symmetry breaking process is not whether the advancing and receding angles converge to the same value after

Received: April 29, 2011
Revised: June 19, 2011
Published: July 05, 2011

some time when a drop is vibrated, but whether it affects the dynamics of motion. While several studies suggest that a drop can attain an energy minimum state after vibration,[22−27] the role of hysteresis on the kinetics of relaxation of a drop has only been addressed recently.[28] In that study, when a drop was vibrated with a Gaussian white noise, its relaxation kinetics was found to be strongly dependent on the strength of the noise. The details of the kinetics as well as the non-Gaussian probability distribution of the displacement fluctuation could satisfactorily be explained only if the effect of hysteresis was taken into account, highlighting its importance in the contact line dynamics.

Our aim here is to study further the plausible role of contact angle hysteresis in the experiments carried out by Daniel et al.[1] We designed an experiment in which surfaces exhibiting varying amounts of hysteresis are used with which to observe the effect of hysteresis on the motion of drops subjected to an asymmetric vibration. The experiments demonstrate and some basic level simulations strongly suggest that contact angle hysteresis could be an essential factor behind the directed motion of drops observed in the experiments of Daniel et al.[1]

EXPERIMENTAL SECTION

A typical experiment was to place a small drop of distilled deionized (DI) water on a solid surface and subject it to lateral asymmetric vibration. In the current experiments, we produced the asymmetric vibration by adding two cosine waves:[29] $A_o(\cos(2\pi\omega t) + 2\cos(4\pi\omega t))$ where A_o is the amplitude of acceleration and ω is the fundamental frequency of vibration. The solid surface was attached on an aluminum platform connected to the stem of a mechanical oscillator (Pasco Scientific, model SF-9324). The asymmetric wave as generated in a waveform editor was sent through the waveform generator (Agilent, model 33120A) to the mechanical oscillator after it was amplified by a power amplifier (Sherwood model no. RX-4105). Accelerometer (PCB Peizotronics, model no. 353B17) driven by a Signal Conditioner (PCB Peizotronics, model no. 482), and connected to an oscilloscope (Tektronix, model no. TDS 3012B), was used to estimate the acceleration of the plate. The accelerometer reading showed that the above asymmetric wave was slightly distorted, when it passed though the oscillator. The asymmetric displacement of the aluminum plate carried the signature of this slight distortion as well (see below). However, as the displacement is periodic, its time average leads to a zero value. The entire setup was placed on a vibration isolation table (Micro-g, TMC) to eliminate the effect of ground vibration. The motion of the drop was recorded with a high-speed camera (Redlake, MotionPro, model 2000) operating at 2000 frames/s. Motion analysis software *MIDAS* was used to track the dynamics of contact line motion of drop.

As mentioned before, our main objective is to study the effect of contact angle hysteresis on the motion of a drop. Hence, we needed surfaces of negligible hysteresis, intermediate hysteresis, as well as strong hysteresis. The hysteresis force acting on the drop depends not only on the difference between the cosine of advancing and receding angles, but also the perimeter of contact between the drop and the substrate. For surfaces with negligible hysteresis, microfibrillated PDMS (Dow Corning Sylgard 184) surfaces were used. The preparation of such surfaces was reported in detail elsewhere.[30] Briefly, the oligomeric component of the Sylgard 184 kit was thoroughly mixed with the cross-linker in a 10:1 ratio by weight followed by degassing it in vacuum for 2 h. The degassed mixture was then cast onto lithographically etched silicon master. These silicon wafers were silanized for easy removal of cured fibrillated PDMS sample. The cast PDMS was then cured at 80 °C for 2 h. The cross-linked PDMS was cooled in dry ice (−78.5 °C) for an hour followed by its removal from the silicon wafer manually. The PDMS surface thus prepared has square fibrils of 10 μm size with fibrillar spacing of 95 μm. The fibrillar spacing here corresponds to the center to center distance between two adjacent fibrils. The height of the fibrils was 25 μm. The low hysteresis fibrillated PDMS surfaces were characterized using the drop rolling method in which a 10 μL drop was placed on a horizontal fibrillated PDMS surface and the angle of inclination of the surface was increased gradually until the drop started to move. The advancing and receding angles of the rolling drop were measured from their video images captured with a computer. These values were 162° and 160°, respectively, with a hysteresis of 2°. The adhesion of water drops to this fibrillated PDMS surface was so low that it proved difficult to transfer the drops onto the surface, as they stuck more to the microsyringe needle rather than to the fibrillated PDMS surface. Use of a very thin microneedle solved this problem.

For the high hysteresis surfaces, a fluorocarbon-coated glass slide and a polystyrene-coated silicon wafer were used. The fluorocarbon surface was prepared by reacting oxygen plasma cleaned microscopic glass slides (Fisher Scientific) with the vapor of 1*H*,1*H*,2*H*,2*H*-perfluorodecyltrichlorosilane (CF_3-$(CF_2)_7$-$(CH_2)_2$-$SiCl_3$, Alfa Aesar). The thickness of the grafted fluorocarbon layer on glass could not be estimated by ellipsometry due to its roughness and close match of the refractive indices of the glass and the grafted layer. The ellipsometric (V-Vase Ellipsometer, J. A. Woollam Co, Inc.) thickness of an equivalent layer on silicon wafers is found to be ∼1.4 nm. The root-mean-square (rms) roughness of the fluorocarbon coated glass slide is found to be 18 nm using atomic force microscopy (Veeco NanoscopeV, Digital Instruments, Metrology Group) over an area of 1 μm × 1 μm. Polystyrene-coated substrates were prepared by spin-casting a 5% solution by weight of polystyrene (MW ∼50 000, Aldrich Chemical Co. Inc.) in toluene on the silicon wafer and drying it for several days. The thickness of polystyrene film was 357 nm with a rms roughness of ∼0.3 nm. Using the drop inflation and deflation methods, the advancing and receding angles were found to be 117° and 103° (hysteresis of 14°), respectively, on the fluorocarbon monolayer coated glass slide, whereas these values were 91° and 68° (hysteresis of 23°), respectively, on the polystyrene surface. For an intermediate hysteresis surface, hydrocarbon and PDMS (trimethylsiloxy-terminated, Gelest Inc., product codes DMS-T22 and DMS-T12) monolayer coated silicon wafers were used. The hydrocarbon monolayer was prepared by reacting plasma cleaned silicon wafer (Silicon Quest International) to the vapor of decyltrichlorosilane (CH_3-$(CH_2)_9$-$SiCl_3$, Gelest Inc.). The thickness of the hydrocarbon monolayer was ∼1 nm with its rms roughness of ∼0.2 nm. The advancing and receding angles measured using drop inflation and deflation method were 107° and 99°, with a net hysteresis of 8°. The PDMS (trimethylsiloxy-terminated) coated silicon wafers were prepared using a method similar to that is described earlier[31] with a slight modification. The silicon wafers (Silicon Quest International) were first cleaned with piranha solution (mixture of concentrated sulfuric acid and 30% hydrogen peroxide in 4:1 volume ratio) for 30 min, followed by rinsing with copious amounts of distilled deionized (DI) water and drying it with ultrapurified nitrogen gas (Praxair Inc.). The silicon wafers were then further cleaned by oxygen plasma (model PDC-32G; Harrick Plasma) at 0.2 Torr for 45 s. Some of these oxygen plasma cleaned silicon wafers were immediately transferred to and immersed in trimethylsiloxy-terminated polydimethylsiloxane (PDMS) (Gelest Inc., DMS-T22, viscosity of 200 cSt, MW 9000−10 000) in a cleaned glass Petri dish. The other remaining oxygen plasma cleaned silicon wafers were immediately transferred to and immersed in a separate clean glass Petri dish containing a different trimethylsiloxy-terminated polydimethylsiloxane (PDMS, DMS-T12 (viscosity of 20 cSt, MW 1600−2400). These Petri dishes were covered and kept in an oven at 100 °C for 24 h. The samples were then cooled to room temperature and dipped in toluene (99.9% pure, ACS grade) for 10 min. Both samples were rinsed with copious amounts of flowing toluene, after which they were dried with ultrapure nitrogen gas. The thicknesses of the grafted PDMS

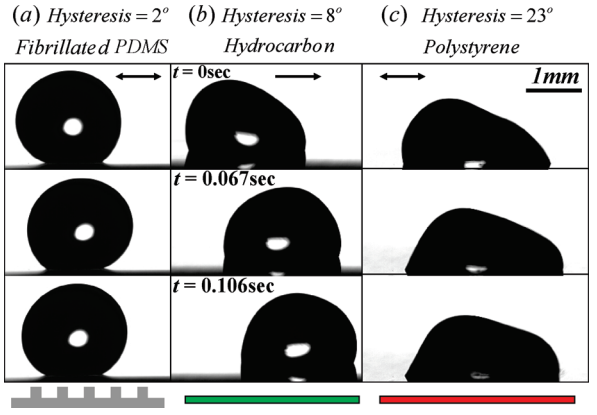

Figure 1. Shape fluctuations of a 4 μL drop subjected to an asymmetric vibration (A_o = 33 m/s^2, ω = 100 Hz) on surfaces of varying magnitude of contact angle hysteresis: (a) fibrillated PDMS (Sylgard 184), (b) hydrocarbon monolayer (decyltrichlorosilane) coated silicon wafer, and (c) polystyrene coated silicon wafer. The amount of contact angle hysteresis increases from panel (a) to (c) as indicated by the magnitude of hysteresis on the top of each panel. The standard deviations in the measurement of the advancing and receding angles are about 1°. The time sequence shown on the middle panel also corresponds to the left and right panels. The drop does not show a net motion on low hysteresis (2°) fibrillated PDMS surface and on the high hysteresis (23°) polystyrene surface, whereas it drifts on the hydrocarbon monolayer coated silicon wafer that has intermediate hysteresis (8°).

films were found to 1.7 nm for DMS-T12 and 5 nm for DMS-T22. The rms roughness values of these surfaces were 0.3 nm for DMS-T12 and 0.4 nm for DMS-T22. The advancing and receding angles measured using the drop inflation and deflation method on silicon wafer coated with PDMS (DMS-T12) were 106° and 95°, respectively, whereas they were 112° and 104° on silicon wafer coated with PDMS (DMS-T22), respectively. The hysteresis (8°) on the latter surface is comparable to that of the hydrocarbon-coated silicon wafer.

EXPERIMENTAL RESULTS

High-speed video (2000 frames/s) captured images of the motion of a small (4 μL drop) water drop on the three surfaces of various degrees of hysteresis (Figure 1) summarize the main point of our finding. The water drop did not exhibit any net drift on the fibrillated PDMS surface with the lowest hysteresis (2°), whereas the drop exhibited significant drift on the hydrocarbon monolayer coated silicon wafer with a somewhat higher hysteresis (8°). The water drop did not, again, move on the polystyrene surface that had high hysteresis (23°). These experimental observations clearly show that some finite amount of hysteresis is essential for directed motion, whereas hysteresis free surface or a surface of large hysteresis are not conducive to such motion. We learned recently that Benilov has made some observations (unpublished) on the effect of hysteresis on drop motion in his theoretical studies that are similar to what we report here.

In order to show the detailed dynamics of the contact lines of the drops on a fibrillated PDMS surface, we carried out the experiments at a relatively high amplitude of vibration (A_o = 97 m/s^2). The 4 μL and 1 μL drops did not exhibit any net drift over several cycles of oscillations (Figure 2). It can be noted in Figure 2 that the net displacement of the plate was larger than those of the drops, suggesting that the drops did not undergo a total slippage on the fibrillated surfaces.

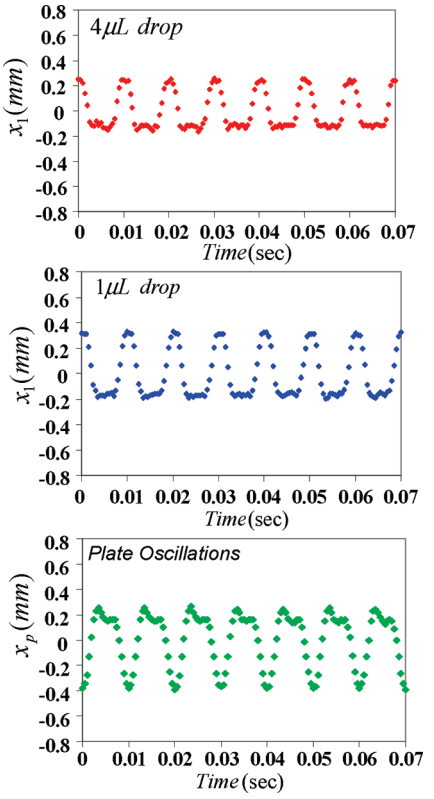

Figure 2. Dynamics of the contact lines of 4 μL and 1 μL water drops on low hysteresis (2°) fibrillated PDMS surface that is subjected to asymmetric vibrations of an amplitude of A_o = 97 m/s^2. The plate oscillations are also shown. The drops do not exhibit any net drift. Here, x_1 corresponds to displacement of contact line of the drop relative to the plate as shown in Figure 5. x_p corresponds to the displacement of the plate with respect to the laboratory frame.

An interesting observation is the so-called "flux reversal" that we observed earlier[1,32] with a different kind of asymmetric vibration and termed it as "polarized ratchet".[32] Here, we carried out an experiment (Figure 3) to accentuate the effect using the asymmetric forcing, where a smaller (1 μL) drop moved downward but a larger (4 μL) drop moved upward on an inclined (15° to the horizontal) hydrocarbon coated substrate under a given frequency and amplitude of vibration. This effect of the drop moving uphill due to asymmetric vibration has also been considered independently in a recent theoretical paper by Benilov.[33] We originally attributed this effect[1] to the difference in the phase of the center of mass oscillations of drops of different volumes, which is illustrated in Figure 4 with respect to the current experiments that shows that the oscillations of the center of masses of 4 μL and 1 μL water drops are out of phase with each other. These results are also relevant to that of Noblin et al.[11] in the context of the uphill motion of a drop by tuning the phase difference of horizontal and vertical vibration of the drop. Detailed explanations of the experimental results of Brunet et al.[10] and Noblin et al.[11] can be found in recent papers by Thiele and John[20] and Benilov and Billingham.[34] At this juncture, we should point out that a solid sphere can also roll on a support with the aid of an asymmetric vibration. Flux reversal can also occur here (see Figure 9). In this case, as the shape fluctuation in the bulk of the sphere is absent, both the rectified motion and flow reversal are caused by a nonlinear rolling friction. A drop

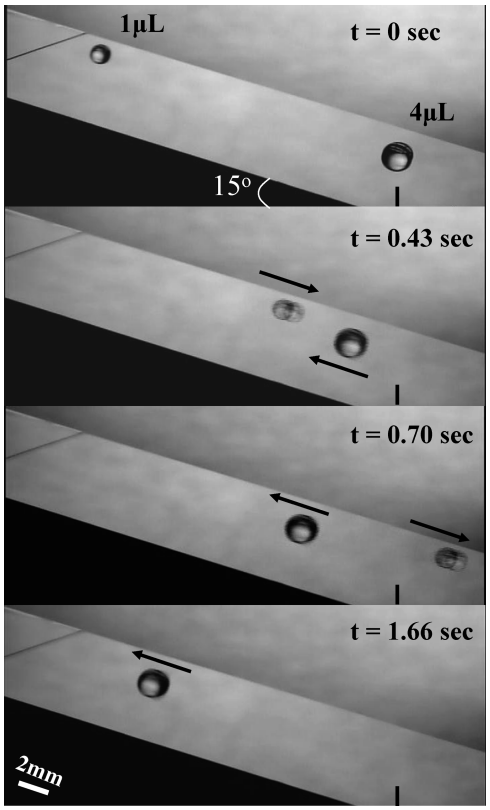

Figure 3. (a) Uphill motion of a 4 μL drop and downhill motion of a 1 μL drop on an inclined hydrocarbon coated silicon wafer subjected to an asymmetric vibration (A_o = 63 m/s^2 and ω = 100 Hz). The inclination of the plate is 15° from the horizontal plane.

does not move on a surface when vibrated with a moderate amount of symmetric periodic vibration. Since these results were published previously,[35] they are not repeated here. A large size drop can however move with the aid of a large-amplitude symmetric vibration (see Figure 10), where the deformation of the drop (presumably) becomes chaotic. This subject is reserved for further analysis and a future publication. In this paper, we focus on the behavior of the drop subjected to only a moderate amount of vibration.

■ COMPARISON OF EXPERIMENTAL AND SIMULATION RESULTS

We now attempt to understand the experimental observations using a simple toy model, in which a drop is approximated as a linear harmonic oscillator as discussed in the earlier publications.[1,3,15,35,36] Since a liquid drop has two degrees of freedom (Figure 5), one at the base and the other at the center of mass, two coupled equations are needed to describe its dynamics. In order to describe the equation of motion of the center of mass of the drop (x_2), an inertial force, a damping force, a spring force, and the imposed oscillatory force are taken into account (eq 1). The inertial force is formally ignored in describing the dynamics of the contact line (x_1). Here, an additional force due to contact angle hysteresis is considered (eq 2).[1]

$$\frac{d^2x_2}{dt^2} + \frac{1}{\tau_B}\frac{dx_2}{dt} + {\omega_o}^2 x_2 = \gamma(t) \qquad (1)$$

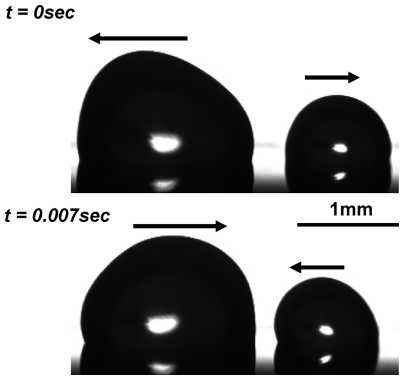

Figure 4. Oscillations of the center of masses of 4 μL and 1 μL water drops subjected to an asymmetric vibrations with A_o = 33 m/s^2 on a hydrocarbon monolayer-coated horizontal silicon wafer. The directions of center mass oscillations are shown by arrows on top of each drop. At t = 0 s, the center of mass of the 4 μL drop moves to the left, whereas that of the 1 μL moves to the right. At t = 0.007 s, the center of mass of the 4 μL moves to the right, whereas that of the 1 μL drop moves to the left. These observations suggest that the oscillations of these drops are out of phase.

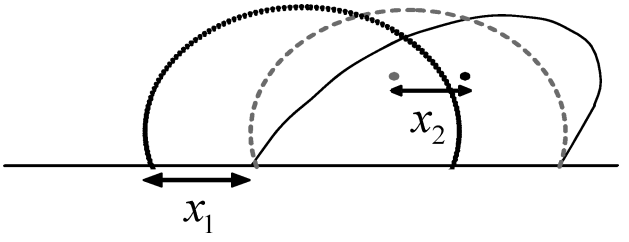

Figure 5. Schematic of the oscillation of a drop on a surface. x_1 indicates the displacement of the contact line relative to the plate and x_2 indicates the displacement of center of mass relative to its undeformed state.

$$\frac{1}{\tau_L}\frac{dx_1}{dt} = {\omega_o}^2 x_2 + \frac{1}{\tau_B}\frac{dx_2}{dt} - \Delta\tanh\left(\alpha\frac{dx_1}{dt}\right) \qquad (2)$$

Here, x_1 and x_2 are the displacements of contact line and center of mass of drop, respectively. τ_B and τ_L are the relaxation times (the ratios of the mass of the drop and kinematic friction coefficient) due to viscous friction in the bulk and near the contact line of the drop. $\omega_o = (k_s/M)^{1/2}$ is the resonance frequency of a drop with M being its mass. The spring constant ($k_s = 2\pi\gamma_{lv}$) is proportional to the surface tension of the liquid, γ_{lv}. $\gamma(t)$ is the imposed acceleration on drop: $-A_o[\cos(2\pi\omega t) + 2\cos(4\pi\omega t)]$. The negative sign indicates that the acceleration of the drop is in opposite direction to that of the plate. $\Delta\tanh(\alpha V)$ is the hysteresis force divided by the mass of the drop, where $V = dx_1/dt$ is the velocity of the contact line. Usually, the hysteresis term enters in the equation of motion as a jump discontinuity, $\sigma(V)\Delta$ with $\sigma(V) = V/|V|$ providing the sign of velocity of the contact line. $\sigma(V)$ takes the values of -1, 0, +1 when $V < 0$, $V = 0$, $V > 0$, respectively, that ensures that the resistance due to contact angle hysteresis always acts against the motion of the contact line of the drop. The difficulty associated with this model is that the signum function is discontinuous at $V = 0$, which results in the discontinuity in force versus velocity relationship. Several approximations can be used to bypass this discontinuity. One approximation

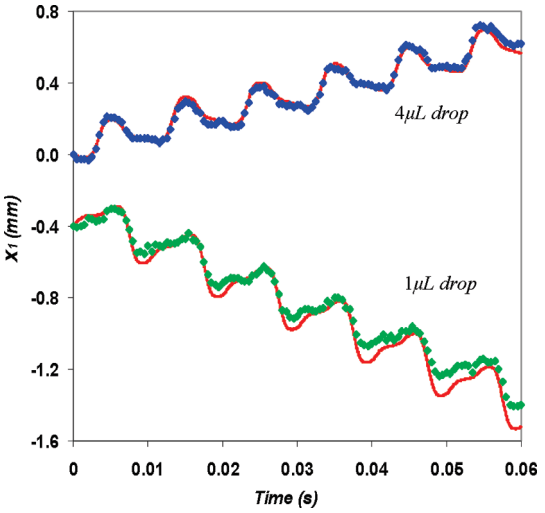

Figure 6. Displacements of the contact lines of 4 μL and 1 μL water drops on a hydrocarbon monolayer coated silicon wafer subjected to an asymmetric vibration with A_o = 33 m/s^2. x_1 corresponds to the displacement of the contact line of the drop relative to the plate as shown schematically in Figure 5. The initial positions of the drops are shifted from zero for clarity of presentation. The blue and green symbols represent the experimental data and the red lines represent the simulation results. We used commercial software *Mathematica* to numerically solve the simultaneous differential eqs 1 and 2. The integration time step is $\Delta t = T/1000$ where T = 0.01 s is time period corresponding to fundamental frequency (ω = 100 Hz) of oscillations.

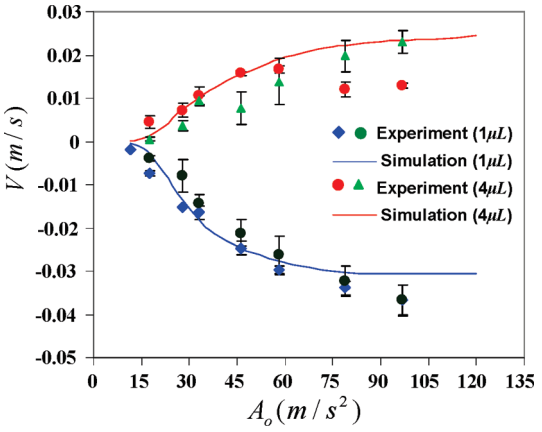

Figure 7. Drift velocities of 1 and 4 μL water drops subjected to asymmetric vibration as a function of amplitude of acceleration (A_o). These experiments are carried out on two different surfaces of similar hysteresis. Blue diamonds and red circles correspond to the data obtained on a hydrocarbon monolayer coated silicon wafer, whereas the dark green circles and the light green triangles correspond to the data obtained on a PDMS monolayer (trimethylsiloxy-terminated, Gelest Inc., product code DMS-T22) coated silicon wafer. As indicated in the text, both of the surfaces used in these experiments have similar hysteresis (8°). The solid blue and red lines correspond to the simulation results.

is to use piecewise continuous functions[37−39] instead of the signum function, and the second is to replace the signum function with another nonlinear function such as tanh (αV), which is widely used in tribology literature[40] involving Coulombic dry friction that has a jump discontinuity similar to that of the wetting hysteresis at V = 0. Here, α is a parameter that signifies how fast the resistive force (acceleration) due to contact angle hysteresis reaches the threshold force (acceleration, Δ) as a function of velocity of contact line. In the limit of $\alpha \rightarrow \infty$, the hyperbolic tangent function is a fair approximation to the signum function. Our objective is to use eqs 1 and 2 in order to gain an understanding of how the drift velocity depends on the threshold value of the hysteresis Δ. However, it is quite challenging to ascertain the various physical parameters (such as relaxation times and threshold hysteresis) needed to carry out such a simulation. In order to estimate these parameters, we examined the high resolution motion of the contact line of water drops (1 μL and 4 μL) on the hydrocarbon surface, which are characterized by a drift velocity, the direction of the drift, amplitude of oscillation, and its phase. The data corresponding to A_o = 33 m/s^2 are shown in Figure 6. All these aspects of the contact line motion could be described from the solutions of eqs 1 and 2 using the values of τ_L, τ_B, and Δ as 0.003 s, 0.002 s, and 35 m/s^2, respectively, for the 1 μL drop, and 0.01 s, 0.008 s, and 10 m/s^2, respectively, for the 4 μL drop. The simulated results are rather insensitive to the value of α as long as it is large enough. We used a value of $\alpha = 50(\text{m/s})^{-1}$, although higher values of α (100 s/m to 200 s/m) produced similar numerical results as well.

We point out that the values of the relaxation times and Δ are in the expected directions for the drops of two different sizes. For example, as the Langevin relaxation time (the ratio of the mass to kinematic friction coefficient, $\tau_L = M/\zeta$) scales with the volume (V) of the drop as $\tau_L \sim V^{2/3}$, we expect τ_L for the larger drop to be at least 2.5 times larger than that of the smaller drop. The value of τ_L needed to describe the motion of the contact line for the larger drop is found to be about 3 times larger than that of the smaller drop. On the other hand, as $\Delta \sim V^{-2/3}$, we expect Δ for the larger drop to be at least 2.5 times smaller than that of the smaller drop. The value of Δ needed to describe the motion of the contact line for the smaller drop is found to be about 3.5 times larger than that of the larger drop. The bulk relaxation time for the larger drop being greater than the smaller drop is also in the expected direction. The values of the parameters τ_L, τ_B, and Δ, as obtained by fitting the experimentally obtained motion of contact lines, are further validated by simulating the trend of drift velocities of the two differently sized drops on two chemically different surfaces (PDMS coated and hydrocarbon coated silicon wafers) but with similar hysteresis at different amplitudes (Figure 7).

The simulation results show that there exists a threshold amplitude of acceleration for each drop ($A_o \sim$ 11.5 m/s^2 for 1 μL drop and $A_o \sim$ 17 m/s^2 for 4 μL drop), below which no drift occurs. The drift velocity increases nonlinearly as the amplitudes of acceleration becomes greater than the threshold. These simulated trends are fairly consistent with the experimental observation of drop motion on these surfaces as summarized in Figure 7.

Inspired by the above agreements, we next estimated the drift velocities of the drops of different sizes as a function of the threshold hysteresis Δ using eqs 1 and 2. The values of the parameters τ_L and τ_B used for this simulation are the same as those used for the hydrocarbon monolayer. This simplification does not pose much of a problem when comparing the experimental data with the simulations for the hydrocarbon, PDMS, and fluorocarbon surfaces as the average contact angles of water on these surfaces are in the range of 103° to 110°. However, they are not supposed to apply rigorously for the fibrillated PDMS and

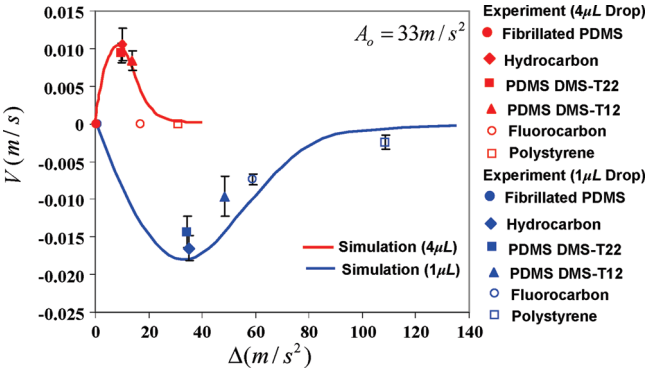

Figure 8. Effect of contact angle hysteresis (Δ) on the drift velocities of 1 μL and 4 μL drops subjected to an asymmetric vibration (A_o = 33 m/s^2, ω = 100 Hz). The solid blue and red lines correspond to the simulation results.

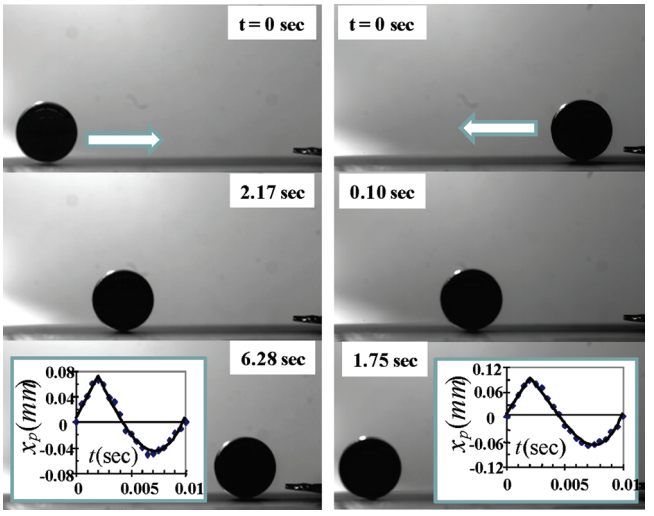

Figure 9. Motion of a steel ball (4 mm) on a horizontal fibrillated PDMS surface due to an asymmetric vibration. The PDMS surface has square fibrils of 10 μm size with fibrillar spacing of 50 μm. The frequency of the vibration is 100 Hz. Left panel shows steel ball moves from left to right when the vibration amplitude is 92 m/s^2. The steel ball moves in opposite direction (right panel) when the vibration amplitude is 142 m/s^2. A nonlinear rolling friction force between steel ball and surface, which has an ascending and descending branch as a function of velocity, seems to be responsible for the symmetry breaking process. One cycle of the displacement of the plate as a function of time is shown in the insets. Previously, Fleishman[29] et al. envisaged a similar flow reversal for the case of small solid object sliding on a solid support.

the polystyrene, other than in a qualitative way, for which the average contact angles of water are 161° and 80°, respectively. The simulation results (Figure 8), nonetheless, are in semiquantitative agreement with the experimental results that show that the drift velocity vanishes as Δ goes to zero; it increases with Δ, reaching a maximum value, and then it decreases as the hysteresis increases further.

The lack of any motion for negligible Δ is due to the absence of the requisite nonlinearity to break the periodic symmetry of the forcing function. On the other hand, with high hysteresis, the applied force is simply not able to depin the contact line from the surface defects. These simulation results are compared with the threshold hysteresis for various surfaces, which are obtained using eq 3

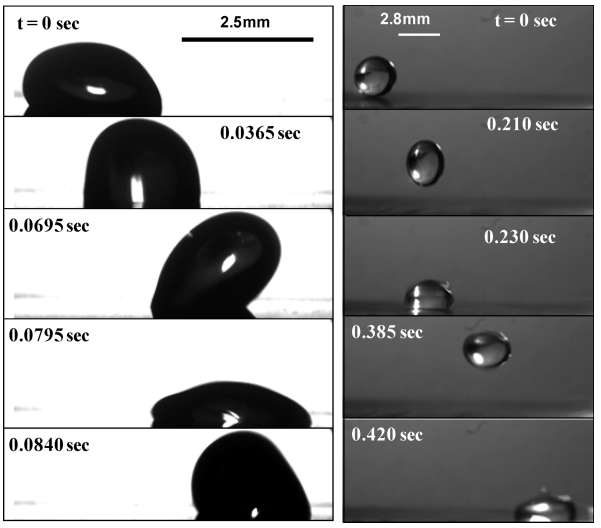

Figure 10. (left panel) A 10 μL drop of water moves on a PDMS (DMS T22) coated horizontal silicon wafer that is vibrated with a sinusoidal vibration parallel to the surface at a frequency of 40 Hz and acceleration amplitude of 100 m/s^2. Significant deformation of the drop shape is observed here. (right panel) A 10 μL drop of water moves on a fibrillated PDMS film when it is vibrated with a sinusoidal vibration parallel to the surface at a frequency of 40 Hz and acceleration amplitude of 90 m/s^2. The drop flies in the air, falls on the surface—only to fly off again. The repetition of this process leads to a net motion of the drop. A vibration induced detachment of a drop from a superhydrophobic surface was reported previously[45] with a vertical vibration. Here, the vibration is horizontal to the surface. Detailed analysis of these effects, including the origin of the symmetry breaking, is under investigation and will be published elsewhere.

and using the measured contact angles.[41]

$$\Delta = \frac{2\pi a \gamma_{lv}(\cos\theta_r - \cos\theta_a)}{M} \quad (3)$$

where a is contact radius of drop, θ_a and θ_r are the advancing and receding contact angles, respectively, M is the mass of the drop, and γ_{lv} is the surface tension of the liquid.

The trend of the experimental results is in reasonable agreement with the simulated results in that the drift velocity varies non-monotonically with Δ, exhibiting extrema at intermediate values of the hysteresis. There are, however, some discrepancies. For example, the simulation predicts the 4 μL water drop to move on the fluorocarbon surface, whereas no motion is observed experimentally. On the other hand, while simulation predicts a 1 μL water drop not to move on the polystyrene surface, a very small drift velocity is observed experimentally. These discrepancies are reminders of the approximate nature of the model used here, having no recourse to the full hydrodynamic description of the problem along with the incompleteness of the details of hysteresis phenomena. In spite of these discrepancies, the main trend is clear in that neither vanishing hysteresis nor large hysteresis is conducive to the drop motion. Some finite but small hysteresis is needed for a drop to move on a surface in the presence of an asymmetric vibration.

CONCLUSIONS

The role played by nonlinear hysteresis needed for a drop to move on a asymmetrically vibrated surface, as proposed earlier[1]

and, here, is formally similar to the nonlinear friction model conjectured by Brunet et al.[10] in explaining the motion of drops due to an oblique vibration. The current study, however, brings to focus the role of hysteresis in definitive terms. The absence of any movement of the drops on the fibrillated PDMS of negligible hysteresis, but its finite drift on the hydrocarbon coated wafer, adequately points to the need for some finite hysteresis to break the symmetry of periodic asymmetric vibration. Very high hysteresis is, however, not conducive to the drop motion, as the strong pinning force cannot not be overcome by a moderate amount of vibration. While the trend of the experimental observations of the effect of Δ on the drop motion is in general agreement with that of the simulation, it is unfortunate that we could not find a surface with a Δ of about 10 m/s^2 to 20 m/s^2 for the 1 μL drop and $\Delta \sim 4$ m/s^2 to 8 m/s^2 for the 4 μL drop amounting to a contact angle hysteresis of about 4° to 6° to fill the gap in the results shown in Figure 8. It is worth noting here that the shape of the oscillating drop on the fibrillated PDMS as well on the polystyrene surface exhibit some noticeable asymmetry, but it does not lead to a net motion of the drop. This observation suggests that asymmetric shape fluctuation may not have a strong role to play in these experiments, although it is quite plausible that its role would be significant for larger-sized drops experiencing much stronger vibrations (see Figure 10). In the problem studied here, a first-order nonlinear force due to hysteresis is responsible for breaking the periodic symmetry, which is formally similar to the Coulombic friction that can also lead to motion of solid objects under periodic or stochastic settings.[15−18] With a solid object, there is no shape fluctuation. Here, the only force that can rectify periodic vibration is a nonlinear friction (see Figure 9). We have performed additional experiments of this type, the details of which will be published elsewhere. Finally, we believe that the results of these studies may have some features that are similar to the vibration induced drift of drops on a surface having a gradient of textures[42,43] or asymmetric wetting.[44]

AUTHOR INFORMATION

Corresponding Author

*E-mail: mkc4@lehigh.edu.

ACKNOWLEDGMENT

We would like to thank Prof. A. Jagota's group at Lehigh University for providing training and the silicon master needed for the preparation of fibrillated PDMS surfaces. We would like to thank Jonathan Longley for Ellipsometric and AFM measurements. We thank Uwe Thiele, Martin Shanahan and Eugene Benilov for valuable comments.

REFERENCES

(1) Daniel, S.; Chaudhury, M. K.; De Gennes, P.-G. *Langmuir* **2005**, *21*, 4240.
(2) Daniel, S.; Chaudhury, M. K. *Langmuir* **2002**, *18*, 3404.
(3) Daniel, S.; Sircar, S.; Gliem, J.; Chaudhury, M. K. *Langmuir* **2004**, *20*, 4085.
(4) Ouellette, J. *Ind. Phys.* **2003**, *9*, 14.
(5) Wu, H.; Wheeler, A.; Zare, R. N. *Proc. Natl. Acad. Sci. U. S. A.* **2004**, *101*, 12809.
(6) Northrup, M. A. *Anal. Chem.* **1998**, *70*, 918.
(7) Darhuber, A. A.; Davis, J. M.; Troian, S. M.; Reisner, W. W. *Phys. Fluids* **2003**, *15*, 1295.
(8) Darhuber, A. A.; Valentino, J. P.; Davis, J. M.; Troian, S. M.; Wagner, S. *Appl. Phys. Lett.* **2003**, *82*, 657.
(9) Daniel, S.; Chaudhury, M. K.; Chen, J. C. *Science* **2001**, *291*, 633.
(10) Brunet, P.; Eggers, J.; Deegan, R. D. *Phys. Rev. Lett.* **2007**, *99*, 144501.
(11) Noblin, X.; Kofman, R.; Celestini, F. *Phys. Rev. Lett.* **2009**, *102*, 194504.
(12) Mogilner, A.; Mangel, M.; Baskin, R. J. *Phys. Lett. A* **1998**, *237*, 297.
(13) Cebiroglu, G.; Weber, C.; Schimansky-G, L. *Chem. Phys.* **2010**, *375*, 439.
(14) Hanggi, P.; Marchesoni, F. *Rev. Mod. Phys.* **2009**, *81*, 387.
(15) Buguin, A.; Brochard, F.; De Gennes, P.-G. *Eur. Phys. J. E* **2006**, *19*, 31.
(16) Fleishman, D.; Klafter, J.; Porto, M.; Urbakh, M. *Nano Lett.* **2007**, *7*, 837.
(17) Mahadevan, L.; Daniel, S.; Chaudhury, M. K. *Proc. Natl. Acad. Sci. U. S. A.* **2004**, *101*, 23(see also the supporting movie 1).
(18) Eglin, M.; Eriksson, M, A.; Carpick, R, W. *J. Appl. Phys.* **2006**, *88*, 091913.
(19) John, K.; Thiele, U. *Phys. Rev. Lett.* **2010**, *104*, 107801.
(20) Thiele, U.; John, K. *Chem. Phys.* **2010**, *375*, 578.
(21) Prakash, M.; Quere, D.; Bush, J. W. M. *Science* **2008**, *320*, 931.
(22) Smith, T.; Lindberg, G. *J. Colloid Interface Sci.* **1978**, *66*, 363.
(23) Andrieu, C.; Sykes, C.; Brochard, F. *Langmuir* **1994**, *10*, 2077.
(24) Nadkarni, G. D.; Garoff, S. *Langmuir* **1994**, *10*, 1618.
(25) Decker, E. L.; Garoff, S. *Langmuir* **1996**, *12*, 2100.
(26) Meiron, T. S.; Marmur, A.; Saguy, I. S. *J. Colloid Interface Sci.* **2004**, *274*, 637.
(27) Marinescu, M.; Urbakh, M.; Barnea, T.; Kucernak, A. R.; Kornyshev, A. A. *J. Phys. Chem. C* **2010**, *114*, 22558.
(28) Mettu, S.; Chaudhury, M. K. *Langmuir* **2010**, *26*, 8131.
(29) Fleishman, D.; Asscher, Y.; Urbakh, M. *J. Phys.: Condens. Matter* **2007**, *19*, 096004.
(30) Glassmaker, N. J.; Jagota, A.; Hui, C. Y.; Noderer, W. L.; Chaudhury, M. K. *Proc. Natl. Acad. Sci. U. S. A.* **2007**, *104*, 10786.
(31) Krumpfer, J. W.; McCarthy, T. J. *Faraday Discuss.* **2010**, *146*, 103.
(32) Dong, L.; Chaudhury, A.; Chaudhury, M. K. *Eur. Phys. J. E* **2006**, *21*, 231.
(33) Benilov, E. S. *Phys. Rev. E* **2010**, *82*, 026320.
(34) Benilov, E. S.; Billingham, J. *J. Fluid. Mech.* **2011**, *674*, 93.
(35) Mettu, S.; Chaudhury, M. K. *Langmuir* **2008**, *24*, 10833.
(36) Equation of this type involving Coulombic friction was first considered by Caughey and Dienes in the context of the motion of a solid object on another under an external stochastic noise.Caughey, T. K.; Diennes, J, K. *J. Appl. Phys.* **1961**, *32*, 2476.
(37) Makkar, C.; Dixon, W. E.; Sawyer, W. G.; Hu, G. Proceedings of the 2005 IEEE/ASME International Conference on Advanced Intelligent Mechatronics, Monterey, California, USA, 24−28 July, 2005.
(38) Cull, S. J.; Tucker, R. W. *J. Phys. A: Math. Gen.* **1999**, *32*, 2103.
(39) Karnopp, D. *ASME J. Dyn. Syst. Measurement and Control* **1985**, *107*, 100.
(40) Andersson, S.; Soderberg, A.; Bjorklund, S. *Tribol. Int.* **2007**, *40*, 580.
(41) Noblin, X.; Buguin, A.; Brochard, F. *Eur. Phys. J. E* **2004**, *14*, 395.
(42) Shastry, A; Case, M. J.; Bohringer, K. F. *Langmuir* **2006**, *22*, 6161.
(43) Reyssat, M; Pardo, F; Quere, D. *Euro. Phys. Lett.* **2009**, *87*, 36003.
(44) Malvadkar, N. A.; Hancock, M. J.; Sekeroglu, K; Dressick, W. J.; Demirel, M. C. *Nat. Mater.* **2010**, *9*, 1023.
(45) Boreyko, J. B.; Chen, C.-H. *Phys. Rev. Lett.* **2009**, *103*, 174502.